

## Analysis of aerodynamic characteristics of racing cars

Viktor Iliev, Marija Lazarevikj, Aleksandar Stojanovski, Martin Oreshkov

*“Ss. Cyril and Methodius” University in Skopje, Faculty of Mechanical Engineering-Skopje,*  
Corresponding Author: Viktor Iliev

### ABSTRACT

The vehicle performance and stability are significantly affected by its aerodynamic properties. Nowadays, the main target of automotive industry is achieving higher vehicle speed or fuel economy. The flow field around a vehicle is complex and characterized by separation which imposes more detailed design procedure to develop a vehicle fulfilling the main objectives. Larger part of the total road resistance arises from the drag thus much scope is left for improving aerodynamic performance by reducing drag force. The same applies for a racing car which requires as better as possible aerodynamic performance at different speed. In this paper, numerical investigation of air flow around a racing car is conducted using CFD technology. Three small-scale models of racing cars are analyzed. The difference in the geometry is in the front wing and the spoiler between two models having same bodywork, while the third model additionally has different body. It is concluded that the shape of the car elements slightly affects the aerodynamic characteristics. The racing car with the lowest drag is selected and the air distribution around it is further studied by analyzing the vector velocity field and the velocity profile change along the flow direction. Next steps can be taken in order to improve geometry in certain locations to avoid turbulence effects and flow separation.

**Keywords** - Racing car, CFD, Drag coefficient, Aerodynamics

Date of Submission: 06-03-2023

Date of acceptance: 19-03-2023

### I. INTRODUCTION

Automotive industry is one of the largest engineering field in the world. Cutting greenhouse gasses as a requirement to decrease global warming effects on one hand, so as the rapid increment of fuel prices on the other hand, imposed the need to minimize fuel consumption of vehicles by enhancing their performance. Major factors influencing the flow field around the vehicle are the boundary layer, flow field separation and drag force. The main aims in developing a vehicle design is to gain maximum efficiency while obtaining lighter weight as possible. The shape of the vehicle body affects the aerodynamic forces acting on it thus design engineers are focusing on reducing drag force by making small changes in the vehicle shape using the aerodynamics concept. Design changes implemented till today are connected to the rear edge of the vehicle and to the addition of passive control devices such as vortex generators and diffusers [1].

The aerodynamic forces exerted on the vehicle body moving through air can be considered by conducting numerical analysis using Computational Fluid Dynamics (CFD) technology. Varun et al. [2] studied the effect of adding a duct to the sedan car roof on its performance. The numerically obtained results using ANSYS Fluent showed decreased drag

coefficient and lower pressure difference between the front and rear end of the modified car model. Damjanovic et al. [3] improved the aerodynamic design of an existing car by increasing the angle between the hood and front windshield and by adding a rear wing. The numerical results from the CFD analysis in Fluent show better airflow distribution around the redesigned model confirmed by the lesser turbulence behind the car. Moreover, higher down force is generated resulting in better stability of the car. Cakir [4] investigated the aerodynamic characteristics of a high speed sedan passenger vehicle with and without spoilers using ANSYS Fluent. The effect of different geometries of spoilers positioned in different locations at the rear end of the vehicle was analyzed. Adding a wing style spoiler achieved 17% drag reduction, 7% down force increase and elimination of the recirculation zone above the rear window. On the other hand, mounting a spoiler to the rear end with no gap between the spoiler and vehicle surfaces, resulted in 6% drag reduction and 17% down force increase. Hassan [5] numerically studied the aerodynamic performance of a vehicle considering different backlight (rear) angle between 0° and 40°. The author determined that the optimal backlight angle is around 30°.

A racing car aims to navigate a track in the shortest time for which consistent and stable aerodynamic performance is needed [6]. In this paper, CFD analysis of air flow around a racing car is performed in order to select a suitable geometry of the vehicle by fulfilling the criteria of obtaining lowest drag possible. The numerical model is prepared for a small-scale racing car model and the simulations are conducted for wind tunnel conditions.

## II. THEORETICAL BACKGROUND

Understanding the air motion around a solid object such as a vehicle requires calculation of forces and moments acting on it. In a symmetrical flow ( $\beta=0$ ), the resulting aerodynamic force  $F_R$  that occurs on a vehicle is determined by three components: lift force  $F_L$ , drag force  $F_D$  and pitching moment  $M$  (Fig. 1).

$$F_R = \sqrt{F_L^2 + F_D^2}$$

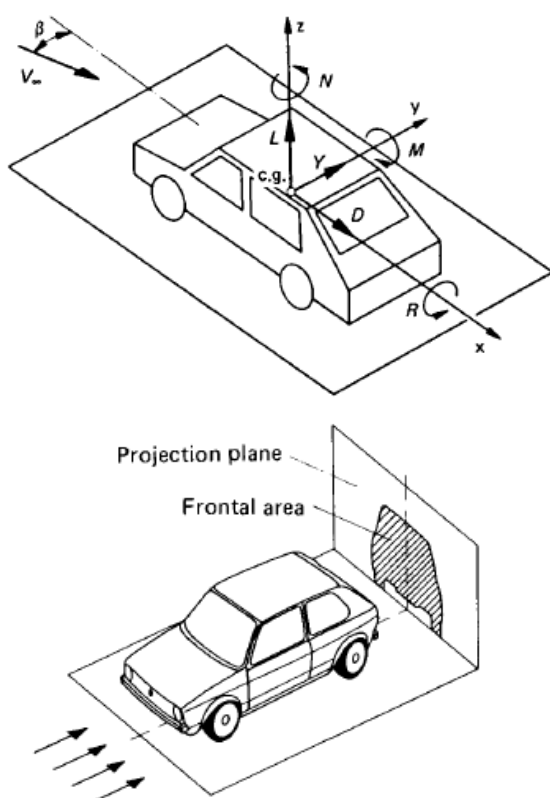


**Fig. 1. Forces and moments acting on a vehicle (left) and definition of frontal area (right)**

The lift force is normal to the air free stream i.e. acting on the body vertically and is produced by the pressure difference between the upper and lower

side of the vehicle. If the lift force is applied in the positive direction, it causes lifting of the vehicle, whereas it results in an excessive wheel down force if applied in negative direction.

The drag force is parallel to the air free stream, resisting the vehicle forward motion and tending to decrease its speed.

The pitching moment reference point is the vehicle center of gravity.

The forces and moments acting on vehicles can be obtained by wind tunnel measurements on full-scale or smaller car models or by CFD analysis. The results do not depend on the actual dimensions if dimensionless coefficients are used, i.e. lift, drag and moment coefficient which are calculated as:

$$C_L = \frac{F_L}{\frac{\rho}{2} v_\infty^2 A}$$

$$C_D = \frac{F_D}{\frac{\rho}{2} v_\infty^2 A}$$

$$C_M = \frac{M}{\frac{\rho}{2} v_\infty^2 A l}$$

where  $\rho$  is the density of the surrounding air,  $v_\infty$  is the air freestream velocity (or vehicle speed) and  $A$  is the projected frontal area of the vehicle [7].

Properties that are usually calculated for the air flow field around the vehicle are velocity, pressure, density and temperature as a function of position and time. Numerical techniques to compute fluid flow around vehicle bodies are based on Navier – Stokes equations which are second order non-linear partial differential equations governing fluid motion and solved by finite volume method. By defining a control volume in the flow field, equations for the conservation of mass, momentum and energy can be used to solve for the properties.

The continuity equation is as follows:

$$\frac{\partial u}{\partial x} + \frac{\partial v}{\partial y} + \frac{\partial w}{\partial z} = 0$$

while the Navier-Stokes equations for the three coordinate axes are:

$$u \frac{\partial u}{\partial x} + v \frac{\partial u}{\partial y} + w \frac{\partial u}{\partial z} = X - \frac{1}{\rho} \frac{\partial p}{\partial x} + \frac{1}{\rho} \left( \frac{\partial \tau_{xy}}{\partial y} + \frac{\partial \tau_{xz}}{\partial z} \right)$$

$$u \frac{\partial v}{\partial x} + v \frac{\partial v}{\partial y} + w \frac{\partial v}{\partial z} = Y - \frac{1}{\rho} \frac{\partial p}{\partial y} + \frac{1}{\rho} \left( \frac{\partial \tau_{xy}}{\partial x} + \frac{\partial \tau_{yz}}{\partial z} \right)$$

$$u \frac{\partial w}{\partial z} + v \frac{\partial w}{\partial z} + w \frac{\partial w}{\partial z} = Z - \frac{1}{\rho} \frac{\partial p}{\partial z} + \frac{1}{\rho} \left( \frac{\partial \tau_{xz}}{\partial x} + \frac{\partial \tau_{yz}}{\partial y} \right)$$

where u, v and w are the x, y and z-component of velocity vector, X, Y and Z are body forces, p is static pressure and  $\tau$  is shear stress [8].

The flow around the vehicle is steady, viscous and turbulent since it is characterized by irregular fluctuations of air velocity in time and space. One of the most used numerical models for modeling and simulating turbulent flow is the standard k- $\epsilon$  model which is a semi-empirical, two-equation model solving two additional transport equation i.e. for the turbulent kinetic energy k and turbulent dissipation  $\epsilon$  both describing the turbulent flow properties.

The transport equations for k and  $\epsilon$  are:

$$\begin{aligned} \frac{\partial}{\partial t}(\rho k) + \frac{\partial}{\partial x_i}(\rho k u_i) &= \\ &= \frac{\partial}{\partial x_j} \left[ \left( \mu + \frac{\mu_t}{\sigma_k} \right) \frac{\partial k}{\partial x_j} \right] + G_k + G_b - \rho \epsilon - Y_M + S_k \end{aligned}$$

$$\begin{aligned} \frac{\partial}{\partial t}(\rho \epsilon) + \frac{\partial}{\partial x_i}(\rho \epsilon u_i) &= \frac{\partial}{\partial x_j} \left[ \left( \mu + \frac{\mu_t}{\sigma_\epsilon} \right) \frac{\partial \epsilon}{\partial x_j} \right] + \\ &+ C_{1\epsilon} \frac{\epsilon}{k} (G_k + C_{3\epsilon} G_b) - C_{2\epsilon} \rho \frac{\epsilon^2}{k} + S_\epsilon \end{aligned}$$

respectively.  $G_k$  represents the generation of turbulence kinetic energy due to the mean velocity gradients.  $G_b$  is the generation of turbulence kinetic energy due to buoyancy.  $Y_M$  represents the contribution of the fluctuating dilatation in compressible turbulence to the overall dissipation rate.  $C_{1\epsilon}$ ,  $C_{2\epsilon}$  and  $C_{3\epsilon}$  are constants.  $\sigma_k$  and  $\sigma_\epsilon$  are the turbulent Prandtl numbers for k and  $\epsilon$ , respectively.  $S_k$  and  $S_\epsilon$  are user-defined source terms.

### III. NUMERICAL SETUP

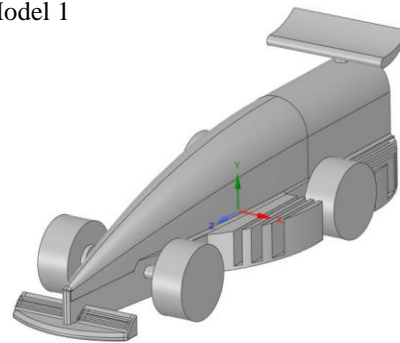
Performing numerical simulations of turbulent flow around vehicle is helpful for prediction of the shape change influence on fluid flow field. Three-dimensional steady turbulent airflow over vehicle is numerically analyzed with the application of ANSYS Fluent. The CFD analysis consists of three parts: preprocessing, processing and post-processing. The preprocessing part consists of geometric model preparation, naming the boundary surfaces and discretization of the numerical flow domain. The processing part consists of choosing a turbulence model, defining boundary conditions and solving.

The post-processing part is comprised of data processing and results presentation.

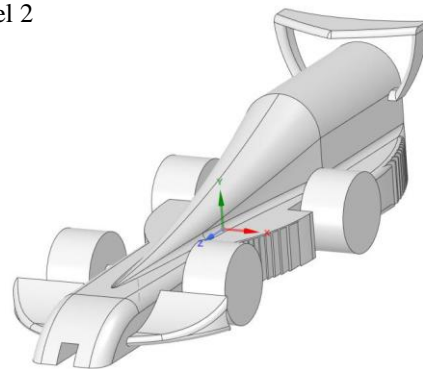
#### Geometry model and named boundary surfaces

Subjects of the numerical analysis are three racing cars further denoted as model 1, model 2 and model 3. The racing car models are shown in Fig. 2.

Model 1



Model 2



Model 3

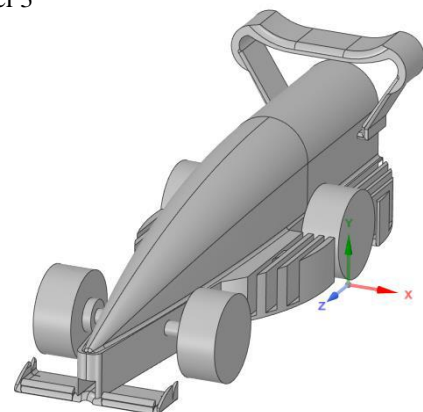


**Fig. 2. Racing cars analyzed: model no.1, 2 and 3**

The differences in the racing car models 1 and 3 are in the geometry of the front wing and the rear wing – spoiler whereas model 2 in addition has different front end bodywork. The length of each car

model is around 200mm. The enclosure and bodies of influence are set up in ANSYS. The length of the flow domain is 1,4m counting the solid object. The dimensions of the flow domain (Fig. 3) are selected so as to provide a uniform and undisturbed air flow in front of the racing car and at the outlet. Bodies of influence are placed around the racing car as a whole and around its wheels in order to define finer mesh in this regions in the next step.

The boundary surfaces needed for the processing part are named as inlet, outlet, sky, ground, side wall, symmetry plane and car outer walls.

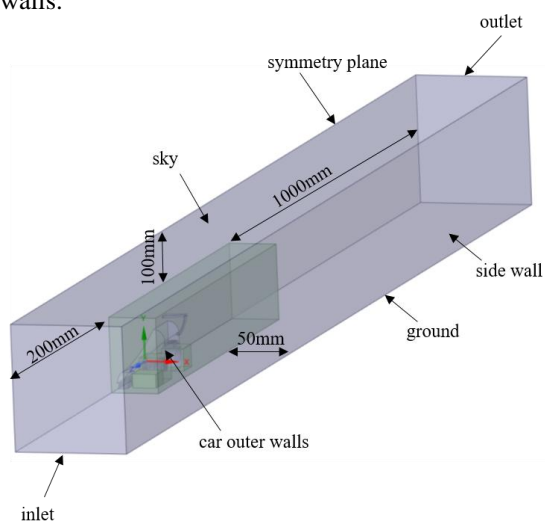


**Fig. 3. Flow domain geometry: basic dimensions and named surfaces**

### Numerical mesh

The numerical grid generated is of polyhedral type because of the complex geometry of the flow domain and the existence of tight zones. In a narrow area around the vehicle body, the mesh is finer since flow occurrence in this contact region with the racing car walls are of most significance. In addition, boundary layers are placed around the outer walls of the racing car and at the upper wall (sky) and lower wall (ground) of the domain. Details of the generated numerical mesh is shown on Fig. 4.

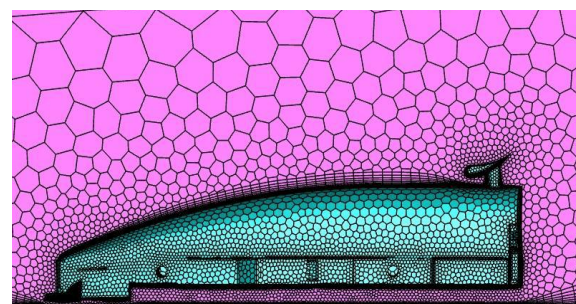
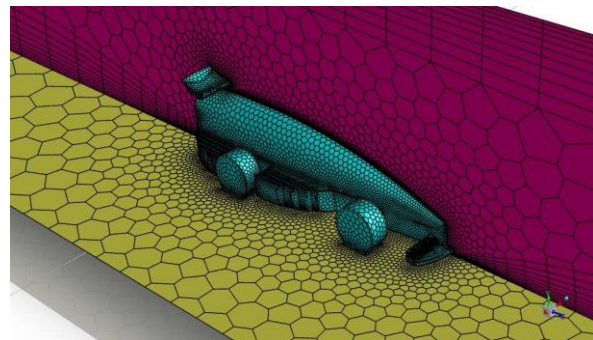


**Fig. 4. Numerical mesh of model no.1**

The rest of the flow domain which is further from the body of influence around the racing car is filled with larger cells since no changes in the flow field are expected thus computational time can be saved.

### Numerical modelling and simulations

Assumptions for the mathematical modelling are made in order to simplify the model and reduce computational effort. Such simplifications consist of assuming no heat transfer between the racing car and its surroundings, constant velocity of air at inlet, incompressibility of the flow i.e. constant density of air.

Boundary conditions used are:

- constant velocity inlet of 25m/s; inlet is placed 0,2m before the racing car front end
- pressure outlet where atmospheric pressure is set
- walls – the surroundings: sky, ground, side wall; the outer walls of the racing car
- symmetry – the plane cutting the racing car and the whole fluid domain in half; the flow field is symmetrical and this reduces the number of nodes.

The boundary conditions and the flow domain geometry are set as for wind tunnel measurements. The standard k-ε model was used for conducting the numerical simulations in this paper.

The convergence of the numerical solution of one racing car model is shown on Fig. 5.

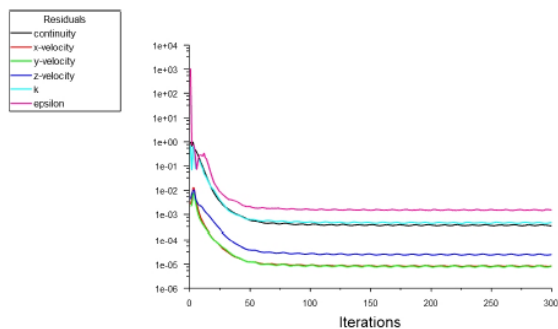


**Fig. 5. Solution convergence – residuals values change vs. iterations**

#### IV. RESULTS AND DISCUSSION

Reducing the aerodynamic drag is the focal point of vehicle aerodynamics. Drag force is proportional to the dynamic pressure of air, the frontal area and the dimensionless drag coefficient. Since the frontal area depends on the design requirements, the efforts to reduce drag are put into decreasing drag coefficient. The aim of this numerical investigation is to select a racing car model with the lowest drag coefficient. The basis of comparison is same for all three models since the same mesh parameters and the same boundary conditions are used.

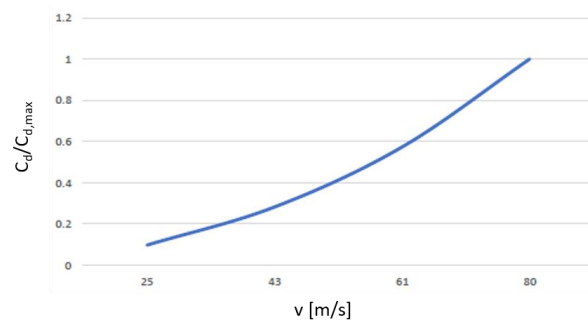
The values of drag coefficient for each model is given in Table 1.

Table 1. Drag and lift coefficient values of racing car models

Model no.	Drag coefficient (-)	Lift coefficient (-)
1	0,563	0,224
2	0,393	0,031
3	0,646	0,073

According to the results obtained for the drag coefficient, model 2 has the lowest value. It is checked that the lift is negative for the model considered which means an excessive downforce exists thus contributing to the racing car stability

Additional numerical simulations are performed for model 2 at different inlet velocities, i.e. Reynolds numbers. The change of the drag coefficient with air speed is shown on Fig. 6. The drag coefficient value is represented on relative scale as a ratio between the actual and the maximum value. Drag coefficient rises with air velocity squared.



**Fig. 6. Drag coefficient change with air speed**

The velocity vectors for model 1, 2 and 3 are given in Fig.7, Fig.8 and Fig.9, respectively. Direction and magnitude of velocity on the symmetry plane is shown. Velocity is highest at the upper bodywork. The presence of rear wing i.e. spoiler mitigates the undesired turbulence.

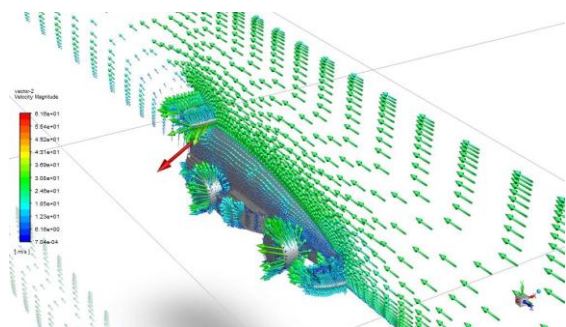


**Fig. 7. Velocity vectors – model 1**

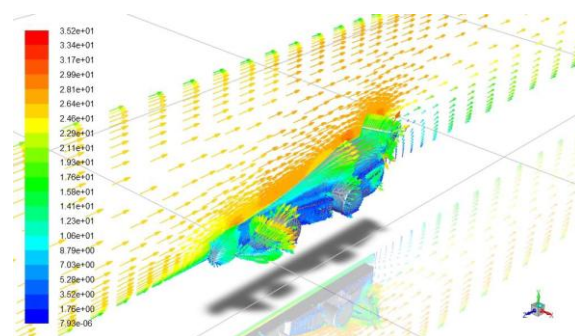


**Fig. 8. Velocity vectors – model 2**

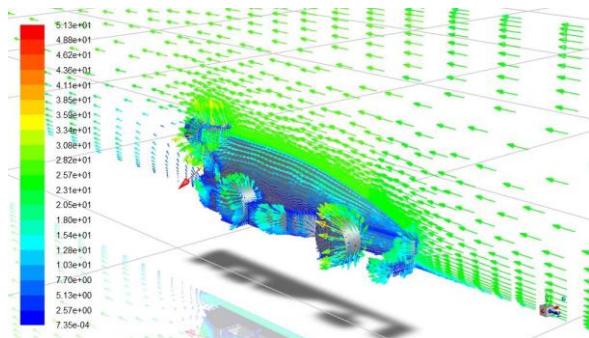


**Fig. 9. Velocity vectors – model 3**

Flow disturbance is also presented by the velocity profile changing along the air flow. Velocity profile is observed at positions shown on Fig. 10. The lines are perpendicular to the air flow.

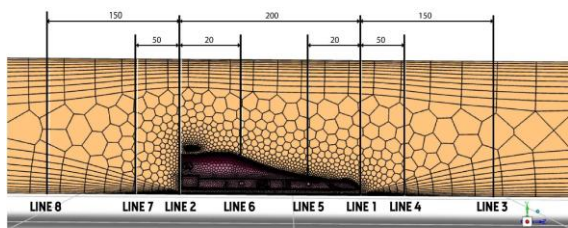
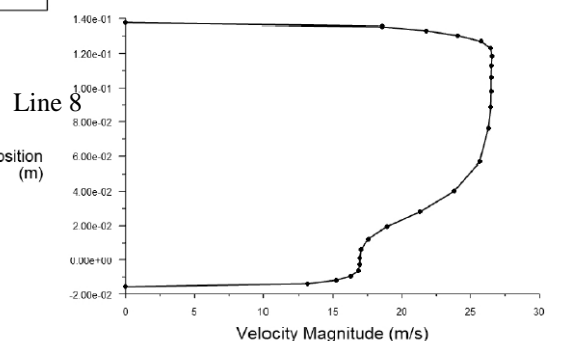
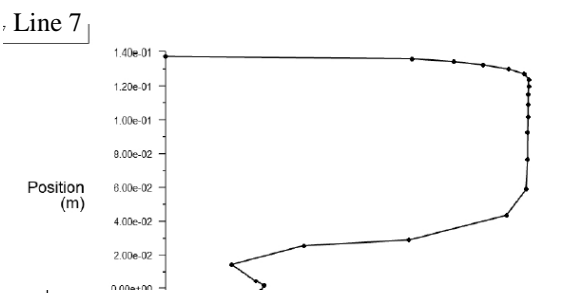
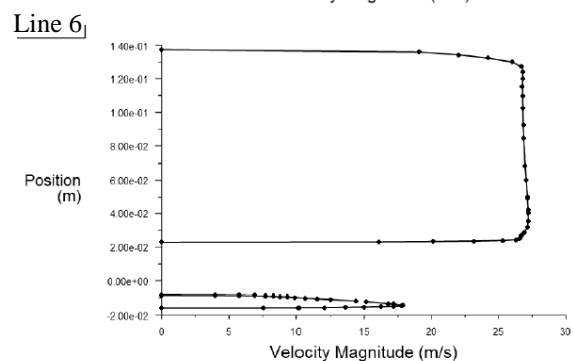
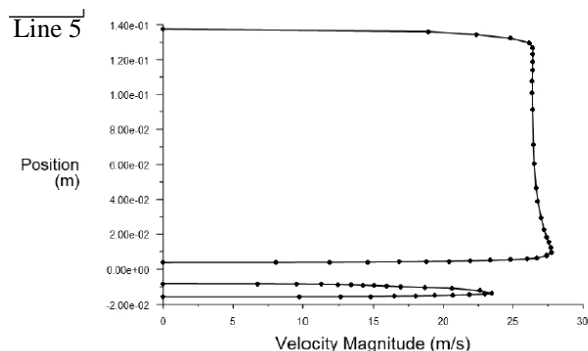
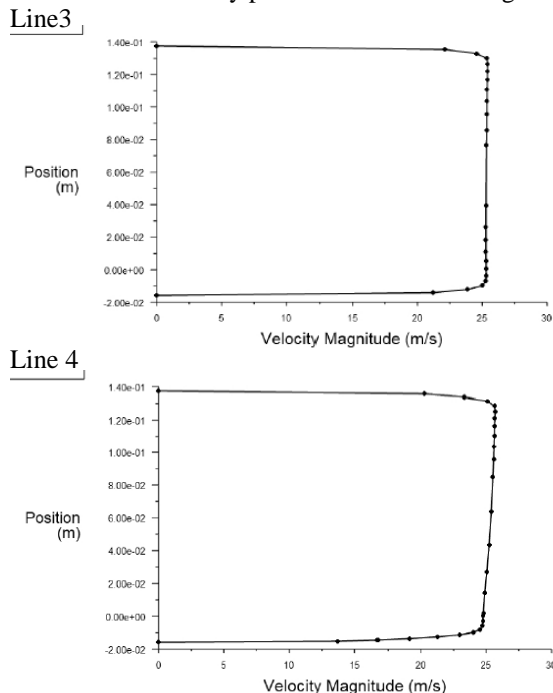


**Fig. 10. Lines on which velocity profile is observed (model 2)**

The obtained velocity profiles are shown in Fig. 11.



It can be seen that there is flow uniformity at 0,15m (line 3) in front of the vehicle. The flow starts to be disturbed in the lower part at 50mm in front of the vehicle (line 4) because of the solid body approaching. At a distance of 20mm from the front end (line 5) and 20mm before the rear end (line 6) of the racing car, the interruption of the flow is noted where the velocity is zero while the flow field above

the car is uniform. The velocity profile under the car i.e. between the chassis and the ground can also be noticed. At a distance 50mm behind the vehicle, the velocity profile is disturbed (line 7), but slowly getting more even when 150mm behind the car.

## V. CONCLUSION

The aerodynamic performance of a racing car can be analyzed in a wind tunnel or using CFD. In this paper, air flow around a racing car is numerically studied. Three geometry models of a racing car are analyzed in order to find the most suitable design. The criteria for selecting a model is lowest drag coefficient as possible. It is concluded that a modification of the front wing and rear wing geometry while having the same bodywork (model 1 and model 3) leads to a small change of the drag coefficient value. Additional alteration of the car body (model 2) leads to slight drag coefficient change. According to the numerical results obtained, the second model has the lowest drag and achieves a negative lift i.e. excessive down force providing higher stability of the vehicle while in motion. Further analysis of flow field around model 2 is conducted by showing velocity vectors for considering turbulence effects and velocity profiles for checking air flow uniformity.

## REFERENCES

- [1] A. Ahmed and M. A. Murtaza, "Cfd Analysis of Car Body Aerodynamics Including Effect of Passive Flow Devices – a Review," *Int. J. Res. Eng. Technol.*, vol. 05, no. 03, pp. 141–144, 2016, doi: 10.15623/ijret.2016.0503030.
- [2] R. Varun, S. Sankar, R. Varma, and K. V. Sreejith, "CFD Analysis of Aerodynamics of Car," *Int. J. Innov. Res. Sci.*, vol. 7, no. 5, pp. 4689–4693, 2018, doi: 10.15680/IJIRSET.2018.0705037.
- [3] D. Damjanović, D. Kozak, M. Živić, Ž. Ivandić, and T. Baškarić, "CFD analysis of concept car in order to improve aerodynamics," *Int. Sci. Expert Conf. TEAM 2010*, vol. 1, no. 2, pp. 63–70, 2011.
- [4] M. Cakir, "CFD study on aerodynamic effects of a rear wing/ spoiler on a passenger vehicle," Santa Clara University, 2012.
- [5] S. Hassan, "Aerodynamics Investigation of Rear Vehicle (Backlight angle)," Teesside University, School of Science and Engineering, 2014.
- [6] L. S. Roberts, J. Correia, M. V. Finnis, and K. Knowles, "Aerodynamic characteristics of a wing-and-flap configuration in ground effect and yaw," *Proc. Inst. Mech. Eng. Part D J. Automob. Eng.*, vol. 230, no. 6, pp. 841–854, 2016, doi: 10.1177/0954407015596274.
- [7] W.-H. Hucho, *Aerodynamics of Road Vehicles: From Fluid Mechanics to Vehicle Engineering*, no. 1. Butterworth-Heinemann, 1987.
- [8] ANSYS Fluent, *Release 12.1: Help Topics*.